PAPER

NJC
www.rsc.org/njc

Trihaloacetic acids: an investigation of steric and inductive ligand effects on the synthesis of $[Mn_{12}O_{12}(O_2CCX_3)_{16}(H_2O)_4]$ single-molecule magnets

Jordi Gómez-Segura,[a] Elsa Lhotel,[b] Carley Paulsen,[b] Dominique Luneau,[c] Klaus Wurst,[d] Jaume Veciana,[a] Daniel Ruiz-Molina*[a] and Philippe Gerbier*[e]

[a] *Institut de Ciència de Materials de Barcelona (CSIC), Esfera UAB, 08193 Bellaterra, Catalonia, Spain. E-mail: dani@icmab.es; Fax: +34 935805729; Tel: +34 935801853*
[b] *Centre de Recherche sur les Très Basses Températures, CNRS, 25 Avenue des Martyrs, BP 166, 38042 Grenoble, France. E-mail: paulsen@grenoble.cnrs.fr; Fax: +33 476885060; Tel: +33 76889038*
[c] *Laboratoire des Multimatériaux et Interfaces, Université Claude Bernard, 43 Boulevard du 11 Novembre 1918, 69622 Villeurbanne, France. E-mail: luneau@pop.univ-lyon.fr; Fax: +33 472431160; Tel: +33 472431418*
[d] *Institut für Anorganische und Theorische Chemie, Universität Innsbruck, Innrain 52a, A-6020 Innsbruck, Austria. E-mail: Klaus.Wurst@uibk.ac.at; Fax: +43(0)512/507-2934; Tel: +43(0)512/507-5145*
[e] *Laboratoire de Chimie Moléculaire et Organisation du Solide, Université Montpellier II, C.C. 007, Place Eugène Bataillon, 34095 Montpellier cedex 05, France. E-mail: gerbier@univ-montp2.fr.; Fax: +33 467143852; Tel: +33 467143972*

Received (in Montpellier, France) 23rd July 2004, Accepted 6th October 2004
First published as an Advance Article on the web 19th January 2005

The preparation of three new single-molecule magnets (SMM), $[Mn_{12}O_{12}(O_2CCX_3)_{16}(H_2O)_4]$, where X = F, Cl or Br, was attempted. Reaction of $[Mn_{12}O_{12}(O_2C^tBu)_{16}(H_2O)_4]$ (**1**) with the carboxylic acid CF_3COOH yielded small black needle-like crystals of complex $[Mn_{12}O_{12}(O_2CCF_3)_{16}(H_2O)_4]\cdot 2.5H_2O$ (**2**). Frequency-dependent out-of-phase ac signals in the range 4–7 K were observed, which indicates that complex **2** functions as an SMM. On the contrary, the use of the bulkier trihaloacetic acids CCl_3COOH and CBr_3COOH is shown to disrupt the formation of the $[Mn_{12}O_{12}(O_2CR)_{16}(H_2O)_4]$ single-molecule magnets, giving rise to the formation of low nuclearity clusters. On the basis of these results and by comparison with the stability of previously described Mn_{12} complexes, an interplay of steric and inductive effects is proposed as the critical factor in determining the thermal stability of these complexes.

Introduction

The discovery of large metal cluster complexes with magnetic properties that are characteristic of nanoscale magnetic particles, such as out-of-phase ac magnetic susceptibility signals and stepwise magnetization hysteresis loops, represented an exciting breakthrough to access high-density information storage devices and quantum computing applications.[1] Even though different families of single-molecule magnets (SMM) based on manganese,[2] nickel,[3] cobalt,[4] iron[5] and mixed metals[6] have been synthesized (*vide supra*), much attention has been focused on the family of molecules based on a dodecamanganese core, denoted in a general way as $[Mn_{12}O_{12}(O_2CR)_{16}(H_2O)_x]$. These complexes possess an $[Mn_{12}(\mu_3\text{-}O)_{12}]$ core, comprising a central $[Mn^{IV}{}_4O_4]^{8+}$ cubane structure held within a non-planar ring of eight Mn^{III} ions by eight $\mu_3\text{-}O_2$ ions, with peripheral ligation provided by sixteen carboxylate groups and three or four H_2O ligands.[7] Small structural variations of the Mn_{12} core induced by environmental and lattice network characteristics have been shown to significantly influence their magnetic properties and quantum tunnelling behaviour. For example, pure Jahn–Teller isomers of a given Mn_{12} complex that crystallize in the same space group and differ only in the identity of one solvent molecule of crystallization, at one position, have been prepared and were shown to exhibit different magnetization relaxation rates.[8] Recent X-ray crystallography studies have also shown that the presence of non-axial isomers in the crystal lattice of Mn_{12} clusters may provide a possible explanation for the intriguing tunnelling behaviour of single-molecule magnets.[9]

To gain knowledge on how subtle structural modifications of the $[Mn_{12}(\mu_3\text{-}O)_{12}]$ structure may influence the stability and magnetic properties of Mn_{12} single-molecule magnets, we were motivated to undertake a systematic investigation of a number of Mn_{12} complexes differing in the nature of the peripheral carboxylic ligands. In this work, we present a detailed study of the ligand series CX_3COOH (X = F, Cl or Br), which exhibits a systematic variation of the volume and Lewis base character. We will show that both effects play an important role in the stability of Mn_{12} complexes.

Results

Synthesis

The synthesis of complexes $[Mn_{12}O_{12}(O_2CCX_3)_{16}(H_2O)_4]$, where X = F, Cl or Br, was attempted following a synthetic methodology recently described by us.[10] Such a methodology is based on the use of complex $[Mn_{12}O_{12}(O_2C^tBu)_{16}(H_2O)_4]$ (**1**) as the starting material for a substitution reaction with the

DOI: 10.1039/b411371c

corresponding carboxylic acid. The presence of *tert*-butyl groups increases significantly its solubility in organic solvents and favours the displacement of the substitution equilibrium to completion due to its dissociation constant.

$$\mathbf{1} + 16\ RCO_2H \rightarrow [Mn_{12}O_{12}(O_2CR)_{16}(H_2O)_4] + 16\ {}^tBuCO_2H \quad (1)$$

Following this approach, reaction of complex **1** with the carboxylic acid CF_3CO_2H yielded small black needle-like crystals of complex $[Mn_{12}O_{12}(O_2CCF_3)_{16}(H_2O)_4]\cdot 2.5H_2O$ (**2**). On the contrary, reaction of carboxylic acids CCl_3CO_2H and CBr_3CO_2H with complex **1** did not yield the corresponding Mn_{12} complexes, even though several treatments were tried. Indeed, surprisingly, ligand substitution reaction of complex **1** with CCl_3CO_2H yielded dark green crystals that were characterized by elemental analysis, spectroscopic techniques and X-ray diffraction as the mixed valence complex $[Mn_3O(O_2CCCl_3)_6(H_2O)_3]\cdot H_2O\cdot C_5H_{12}$ (**3**).

Reaction of complex **1** with CBr_3CO_2H yielded dark red single crystals that were isolated and characterized by elemental analysis, spectroscopic and X-ray diffraction techniques as the mixed valence complex $[Mn_6O_2(O_2CCBr_3)_{10}(H_2O)_3(Et_2O)]\cdot Et_2O$ (**4**). Along the course of our work, it was also found that different batches of **4** were altered with small amounts of an impurity, which was characterized by elemental analysis and spectroscopic techniques as complex $[Mn_3O(O_2CCBr_3)_6(H_2O)_3]$ (**5**). Most likely, decomposition of the Mn_{12} cluster initially yields the Mn_3 complex **5**, which in turn aggregates to yield the $[Mn_6O_2]^{10+}$ core, as previously described in the literature.[11]

X-Ray crystallography

Complex $[Mn_{12}O_{12}(O_2CCF_3)_{16}(H_2O)_4]\cdot 2.5H_2O$ (**2**) crystallizes in the triclinic *P*-1 space group with two molecules in the unit cell. Moreover, two and a half uncoordinated water molecules per Mn_{12} complex were found in the unit cell: two water molecules are located in general positions, whereas the third one is located on a symmetry centre. As shown in Fig. 1, complex **2** possesses an $[Mn_{12}(\mu_3\text{-}O)_{12}]$ core that could, essentially, be superimposed onto other Mn_{12} complex cores: namely, a central $[Mn^{IV}{}_4O_4]$ cubane surrounded by a nonplanar ring of eight Mn^{III} atoms that are connected to the cubane by eight $\mu_3\text{-}O^{2-}$ ions. Peripheral ligation is provided by sixteen CF_3COO^- carboxylate groups and four H_2O molecules that are bound to Mn(11), Mn(21) and Mn(9) in a 1 : 1 : 2 topology.[12]

The crystal packing of complex **2** (see Fig. 1) shows crystallographically independent chain-like structures, aligned along the *a* axis, intercalated with water molecules. Each chain exhibits a zig-zag alternation of Mn_{12} moieties, connected through one short F–F contact (2.932 Å) and hydrogen bonds between one interstitial and two coordinated water molecules (2.808 Å). A second interstitial water molecule is hydrogen-bonded to one carboxylic group (2.872 Å).

The ORTEP plots of complexes $[Mn_3O(O_2CCCl_3)_6(H_2O)_3]\cdot H_2O\cdot C_5H_{12}$ (**3**) and $[Mn_6O_2(O_2CCBr_3)_{10}(H_2O)_3(Et_2O)]\cdot Et_2O$ (**4**) are shown in Fig. 2. The molecular structure of complex **3** exhibits a characteristic μ_3-oxo-bridged trinuclear manganese core, previously described in the literature.[13] The structure consists in a μ_3-oxo-bridged trinuclear manganese structure in which each manganese atom has a distorted octahedral environment, composed of the μ_3-oxo atom, four oxygen atoms from bridging carboxylate groups and one H_2O molecule. The molecular structure of complex **4** is similar to those previously described for related Mn_6 complexes[14] and consists in six Mn atoms arranged as two edge-sharing tetrahedra. At the centre of each tetrahedron lies a $\mu_4\text{-}O^{2-}$ ion. Peripheral ligation is accomplished by ten bridging carboxylate ligands, three terminal water molecules and one Et_2O molecule.

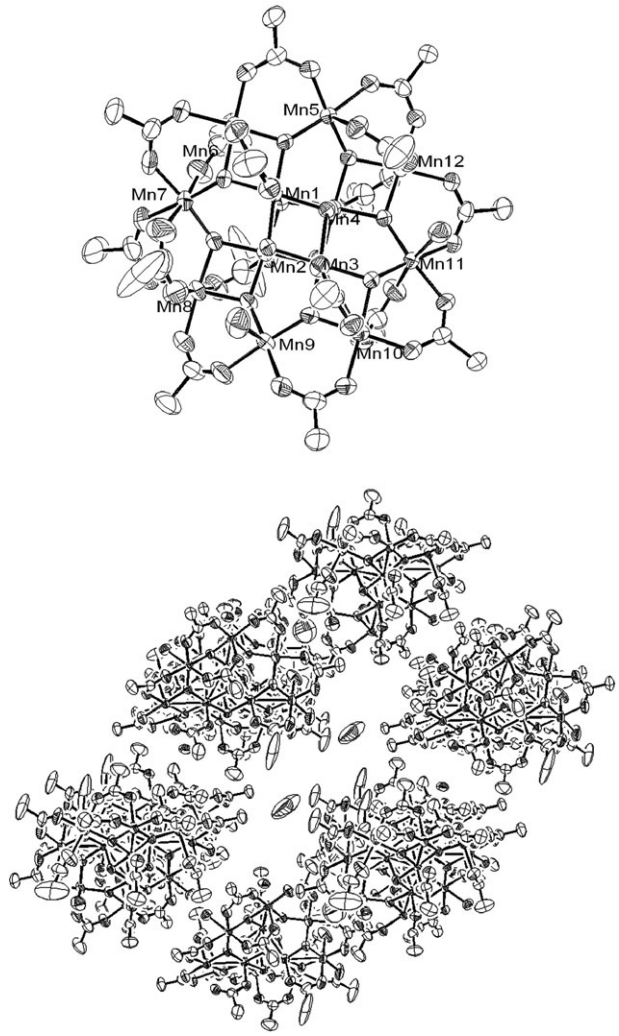

Fig. 1 ORTEP plot of complex $Mn_{12}O_{12}(O_2CCF_3)_{16}(H_2O)_4]\cdot 2.5H_2O$, **2** (top) and its corresponding crystal packing (bottom). Hydrogen and fluorine atoms are omitted for clarity.

Magnetic properties

Ac magnetic susceptibility data were obtained for a polycrystalline sample of complex **2** in the 2.5–10 K range with a 1 Oe ac field oscillating in the frequency range 2.11–57.7 Hz and an external magnetic field held at zero. The frequency-dependent out-of-phase ac peaks are shown in Fig. 3. Complex **2** exhibits frequency-dependent out-of-phase ac signals in the range of 3–6 K characteristic of SMM.[15] The nonzero value of χ_{ac} at low temperatures could be tentatively attributed to a small impurity containing Mn(II) ions and/or the presence of a small fraction of an isomeric form of complex **2**, exhibiting a faster magnetic relaxation.

Ac magnetic susceptibility data not only can be used to determine whether a molecule functions as an SMM, but also to obtain the effective energy barrier (U_{eff}) for magnetization relaxation. Magnetization relaxation parameters, namely the effective energy barrier (U_{eff}) and the relaxation time (τ_0), were extracted from the fit to the Arrhenius equation (eqn. 2) of the plot $\ln(\tau)$ *versus* T_{max}, where $\tau = 1/2\pi\nu$ and T_{max} is the temperature at which the χ'' peak maximum is observed. The best fit gave values of 62 K for U_{eff} and 1.7×10^{-8} s for τ_0, both within the range of those observed for other members of the Mn_{12} family.

$$\frac{1}{\tau} = \frac{1}{\tau_0}\exp(-U_{eff}/kT) \quad (2)$$

The observation of pronounced magnetization hysteresis loops at very low temperatures is also an experimental manifestation

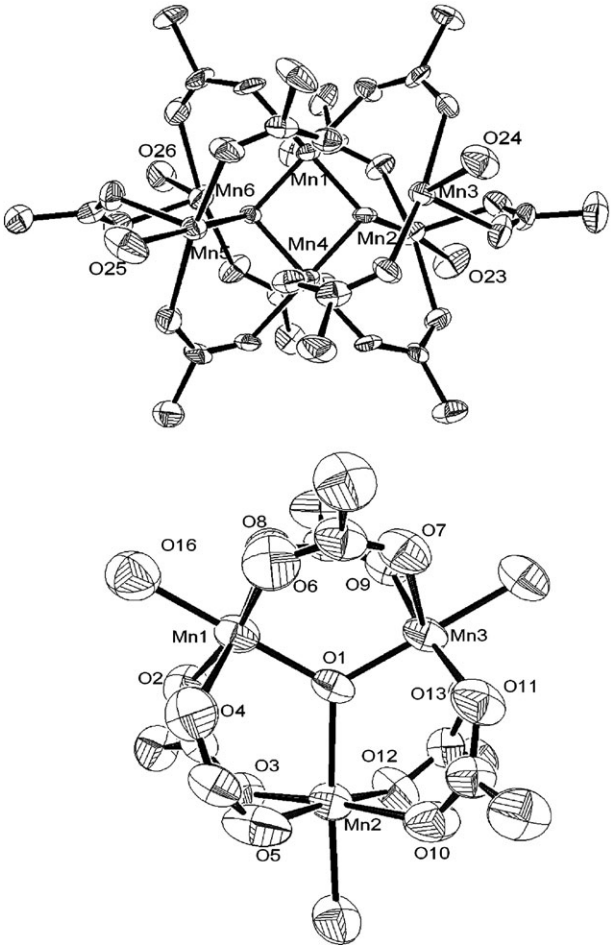

Fig. 2 ORTEP plots of the core of complexes $[Mn_6O_2(O_2CCBr_3)_{10}(H_2O)_3(Et_2O)]\cdot Et_2O$, **4** (top), and $[Mn_3O(O_2CCCl_3)_6(H_2O)_3]\cdot H_2O\cdot C_5H_{12}$, **3** (bottom). Hydrogen atoms and organic peripheral groups are omitted for clarity.

of single-molecule magnetism behaviour. Magnetization hysteresis data were obtained for a polycrystalline sample of complex **2** at 2.5 K. The sample was oriented so that the axial anisotropy axis of the molecule was parallel to the external field. The sample was first subjected to a +4.0 T field, then the field was swept down to −4.0 T, and cycled back to +4.0 T. The value of the magnetization observed at 4.0 T is consistent with an $S = 10$ ground state ($M = 20\ \mu_B$). As the field is decreased from +4.0 to 0 T, there is a first step at zero field and successive steps are observed at a field interval of $\Delta H \simeq 5$ kOe.

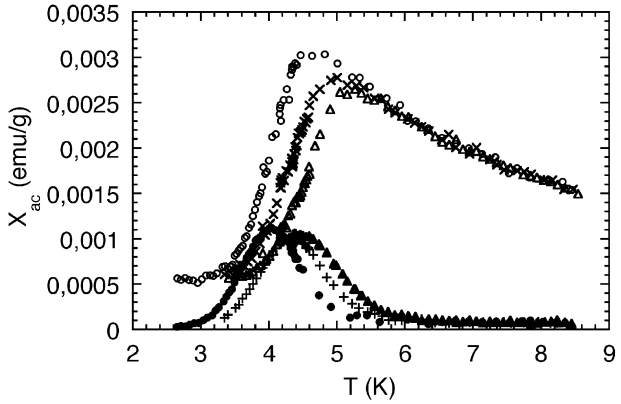

Fig. 3 Ac magnetic measurements for complex **2** in a 1.4 Oe ac field oscillating at the frequencies (○, ●) 2.11, (□, ■) 5.7 and (△, ▲) 11.1 Hz, with no applied dc field. Open symbols represent the in-phase susceptibility χ' and solid symbols represent the out-of-phase susceptibility χ''.

If all the molecules changed their direction of magnetization by thermal activation over the barrier, then the hysteresis loop would be a smooth function with no steps. The above observations can be explained in terms of resonance quantum mechanical tunnelling in the magnetization direction.[16]

Variable-temperature magnetic susceptibility data for complexes **3** and **4** over the range 1.8–300 K, under an applied magnetic field of 1000 Oe, were obtained. Since triangular mixed-valence Mn_3O experiences spin frustration, their ground state may vary between $S = 1/2$ and $S = 3/2$, depending on ligand changes.[17] In this work, complex **3** is characterized as having an $S = 3/2$ ground spin state rather than the $S = 1/2$. On the other hand, the χT *versus* T plot of complex **4** showed the presence of antiferromagnetic interactions between the manganese ions, with a decrease in its value upon decreasing the temperature. Such antiferromagnetic interactions lead to an $S = 0$ ground state, as confirmed by magnetization *versus* field measurements.

Thermal stability

Thermogravimetric analysis (TGA) studies carried out on a polycrystalline sample of complex **2** under an air flow are shown in Fig. 4. The TG curve exhibits an initial smooth weight loss of 3% in the temperature range 80–110 °C, which is attributed to the elimination of the three interstitial water molecules (theoretical weight loss: 2%). A further increase of the temperature produced a more pronounced two-step weight loss (onset temperature *ca.* 130 °C) associated to an additional weight loss of approximately 68.3%. This step, which is the final exothermal degradation, yielded a solid that was identified as Mn_3O_4 from its powder X-ray pattern (theoretical weight loss: 67.1%).

TGA curves of complexes **1** and $[Mn_{12}O_{12}(O_2CCH_3)_{16}(H_2O)_4]\cdot 4H_2O\cdot 2CH_3CO_2H$ (**6**) were also studied for comparison purposes (see Fig. 4).[18] Both complexes exhibit a weight loss in the temperature range 70–170 °C that is attributed to the elimination of $4H_2O + 2CH_3CO_2H$ (obs.: 11.6%, calcd: 9.3%) for complex **6** and $4H_2O + 1\ ^tBuCO_2H$ (obs.: 7.0%, calcd: 6.8%) for complex **1**. An increase in the temperature evidenced that complexes **1** and **6** remain stable up to at least *ca.* 150 and 180 °C, respectively. Above these temperatures, additional weight losses of 48.2% for **1** and 38.0% for **6** are also observed. These are associated to the final exothermal degradation to yield, in both cases, a dark-brown solid identified as Mn_3O_4 from its powder X-ray pattern. Interestingly, examination of the temperatures at which Mn_{12} core degradation takes place (**2**: 130 °C, **1**: 150 °C, **6**: 180 °C) evidences a close relationship between the chemical nature of the peripheral ligands and the thermal stability of the complex.

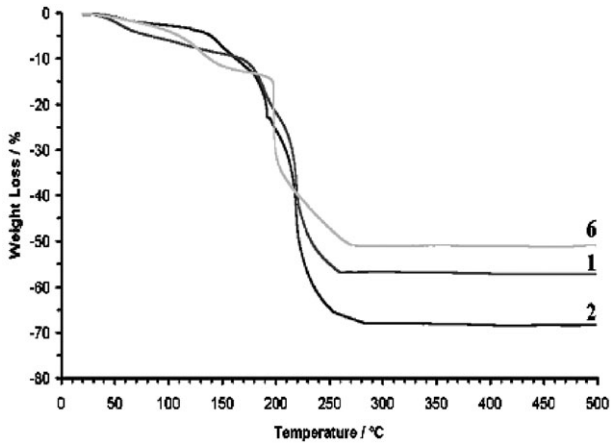

Fig. 4 TG curves of complexes **1**, **2** and **6** in the temperature range 20–500 °C under an air flow.

Discussion

Reaction of complex **1** with CF_3COOH yields complex **2**, whose structure and magnetic properties are similar to those already described for most Mn_{12} complexes so far reported. Nevertheless, when its thermal behaviour is compared to those of complexes **1** and **6**, clear differences are observed. Hence, the question is: what is such a different thermal stability due to? Is it from inductive and/or steric effects? To give more insight into these questions, the role of the steric repulsions has been analyzed first. Space-filling diagrams of complex **1**, obtained from geometry optimization,[9] and of complexes **2** and **6**, obtained from X-ray data,[20] are shown in Fig. 5. As can be seen, in the case of complex **2**, the larger van der Waals radius of fluorine atoms, in comparison to the small hydrogen atoms present in complex **6**, induces an increase of steric congestion, more visible for the axial than the equatorial ligands. This effect is even more remarkable in complex **1**, considering the larger van der Waals radius of methyl groups. In this case, short H···H distances (*ca.* 2 Å), that is, slightly lower than the sum of the van der Waals' radii, are found between axial ^{t}Bu, whereas the longer ones (*ca.* 3 Å) are found within the equatorial groups. Therefore, the relative thermal stability of the Mn_{12} complexes **6** (R = Me) > **1** (R = ^{t}Bu) > **2** (R = CF_3) does not correlate with the increase in the volume of the R groups: **1** (R = ^{t}Bu) > **2** (R = CF_3) > **6** (R = Me), see Table 1.

The relative thermal stability of Mn_{12} complexes **6** (R = Me) > **1** (R = ^{t}Bu) > **2** (R = CF_3) does not correlates with an increase in their Lewis base character either: **6** (R = Me) ≈ **1** (R = ^{t}Bu) > **2** (R = CF_3). The stronger electron-withdrawing ability of fluorine atoms makes the CO_2^- group less basic, thus reducing the electron density on the metal centres. As an apparent consequence, the more electron-deficient Mn_{12} complex **2** appears to be less thermally stable than its analogues **1** and **6**, for which the basic character of the carboxylate ligands is considerably larger (see Table 1). However, this consideration is no longer effective once the thermal stabilities of complexes **1** and **6** are compared. Even though the Lewis base characters of both carboxylate ligands CX_3COO^- [X = Me (**1**) and H (**6**)] are quite similar, as illustrated in Table 1, complex **6** is considerably more stable than complex **1**, a fact that has been attributed to an increase in steric congestions. According to these results, the thermal stability of Mn_{12} complexes clearly depends on an interplay between steric and ligand inductive effects.

Such an interplay becomes even more evident in the distinct behaviour of the CCl_3COOH and $C(CH_3)_3COOH$ ligands. Whereas the use of $C(CH_3)_3COOH$ yields complex **1**, stable up to 150 °C, the use of CCl_3COOH directly leads to the formation of lower nuclearity complexes.[21] To explain such divergence, differential inductive electronic effects between the carboxylic ligands must be invoked, since both ligands exhibit similar dimensions. Finally, the combination of a considerable acidity and a very large volume in CBr_3CO_2H also leads to the formation of low nuclearity Mn_3 and/or $[Mn_6O_2]^{10+}$ clusters.[22]

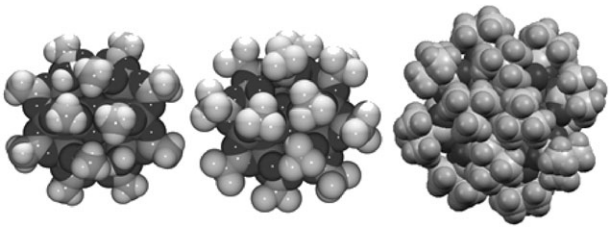

Fig. 5 Space-filling diagrams representing, from left to right: $[Mn_{12}O_{12}(O_2CCH_3)_{16}(H_2O)_4]\cdot 4H_2O\cdot 2CH_3CO_2H$ (**6**), $Mn_{12}O_{12}(O_2CCF_3)_{16}(H_2O)_4]\cdot 2.5H_2O$ (**2**) and $[Mn_{12}O_{12}(O_2C^tBu)_{16}(H_2O)_4]$ (**1**).

Table 1 van der Waals volumes of the RCOOH ligands, pK_a values and temperatures of decomposition (T_d) of the corresponding Mn_{12} complexes

R	Volume/Å^{3a}	pK_a ^{b}	Mn_{12}	T_d /°C
CBr_3	92.8	2.13	No	—
CCl_3	71.0	1.10	No	—
$C(CH_3)_3$	70.7	4.96	Yes	150
$CHCl_2$	56.2	1.37	Yes	110
CF_3	34.1	0.67	Yes	130
CH_3	26.9	4.79	Yes	180

[a] Calculated using Hyperchem QSAR Properties Software, v. 7.5, Hypercube, Inc. [b] Calculated using Advanced Chemistry Development (ACD) Software, Solaris, v. 4.67.

Experimental

All chemicals and solvents were used as purchased. Preparations and manipulations were done under aerobic conditions. Microanalyses were performed by the Servei d'Anàlisi Química of the Universitat Autónoma de Barcelona. The FT-IR spectra were collected on a Perkin Elmer spectrometer on KBr pellets in the range 400–4000 cm^{-1}. $[Mn_{12}O_{12}(O_2C^tBu)_{16}(H_2O)_4]$ (**1**) was prepared following the methodology previously described[10] and the resulting complexes **2**, **3** and **4**, obtained by ligand-substitution reactions, were characterized by elemental analysis, spectroscopic techniques and X-ray diffraction.

Syntheses

$[Mn_{12}O_{12}(O_2CCF_3)_{16}(H_2O)_4]\cdot 2.5H_2O$ (2). To a solution of **1** (0.100 g, 0.039 mmol) in dichloromethane (5 ml) was added CF_3CO_2H (0.179 g, 1.570 mmol); the resulting solution was stirred for a few minutes. Direct crystallization was achieved by slow diffusion of *n*-heptane (5 ml) into this solution. The resulting black needle-shaped crystals were collected by filtration, washed with hexane and dried on the fritted glass filter. FT-IR (KBr, cm^{-1}): 2979 (m); 1674 (s); 1485 (s); 1427 (m); 848 (m); 795 (m); 725 (m); 623 (m). Anal. calcd for $C_{32}H_{14}F_{48}O_{51}Mn_{12}$: C 13.80, H 0.51; found: C 14.03, H 0.53.

$[Mn_3O(O_2CCCl_3)_6(H_2O)_3]\cdot H_2O\cdot C_5H_{12}$ (3). **1** (250 mg, 0.098 mmol) was dissolved in 15 ml of CH_2Cl_2. Subsequently, an excess (40 : 1) of CCl_3CO_2H was added and the reaction mixture was stirred for a few minutes. The filtered solution was layered with pentane and, after full diffusion, was left undisturbed at room temperature in an open Erlenmeyer flask to afford X-ray quality needle-shaped crystals. FT-IR (KBr, cm^{-1}): 3419 (m); 1691 (s); 1683 (s); 1615 (m); 1362 (s); 850 (s); 837 (s); 747 (s); 687 (s). Anal. calcd for $C_{17}H_{20}Cl_{18}O_{17}Mn_3$: C 15.71, H 1.55; found: C 14.19, H 1.55.

$[Mn_6O_2(O_2CCBr_3)_{10}(H_2O)_3(Et_2O)]\cdot Et_2O$ (4). The same procedure as for compound **3** was carried out with an excess (40 : 1) of CBr_3CO_2H. **4** was crystallized from the filtered solution in ethyl ether layered with *n*-heptane. FT-IR (KBr, cm^{-1}): 3401 (m); 1648 (s); 1594 (m), 1358 (s), 771 (m); 722 (m); 609 (m). Anal. calcd for $C_{28}H_{26}Br_{30}O_{27}Mn_6$: C 9.55, H 0.74; found: C 8.62, H 0.79.

X-Ray crystallography

X-Ray quality crystals were obtained by recrystallization and mounted on a Bruker Smart CCD diffractometer equipped with a normal focus monochromated molybdenum target X-ray tube. Crystal data were collected and processed for reduction and absorption with the SAINT software.[23] The

Table 2 Crystal data, data collection and refinement parameters for **2**, **3** and **4**

	2	**3**	**4**
Formula	$C_{32}H_{14}F_{48}Mn_{12}O_{51}$	$C_{17}H_{20}Cl_{18}Mn_3O_{17}$	$C_{28}H_{26}Br_{30}Mn_6O_{27}$
Crystal system	Triclinic	Triclinic	Triclinic
Space group	*P*-1	*P*-1	*P*-1
a/Å	15.7890(8)	10.6317(6)	13.8846(5)
b/Å	19.5781(10)	13.5792(5)	14.8256(4)
c/Å	20.0640(10)	17.0719(9)	21.8859(7)
α/°	95.6100(10)	78.218(3)	102.610(2)
β/°	105.6670(10)	76.225(2)	92.898(2)
γ/°	106.9330(10)	78.187(3)	113.902(2)
U/Å^3	5607.1(5)	2311.6(2)	3970.4(2)
Z	2	2	2
T/K	298(2)	233(2)	293(2)
Obs. reflections	36065	4573	6240
R_{int}	0.0212	0.0259	0.0572
R_1 [$I > 2\sigma(I)$]	0.0623	0.0732	0.0650
wR_2 (all data)	0.2152	0.2097	0.1662

structures were solved with the SHELXTL software.[24] All nonhydrogen atoms were refined with anisotropic thermal parameters. The hydrogen atoms were included in the final refinement model in calculated positions with isotropic thermal parameters although there are hydrogen atoms missing from each refinement. Crystal and refinement data are summarized in Table 2.†

Magnetic measurements

Ac and dc magnetic measurements were carried out on a Quantum Design MPMS SQUID magnetometer equipped with a 5.5 T magnet. The operational range of temperature corresponds to 1.8–300 K with an ac field range of 0–3.8 Oe and an oscillating frequency range of 0–150 Hz. Magnetic measurements at low temperature were performed on a high field (up to 8 T) SQUID magnetometer, developed at CRTBT (CNRS), equipped with a miniature dilution refrigerator, which allows measurements in the temperature range 0.1–8 K. Absolute values of the magnetization and the ac susceptibility are obtained by the extraction method.

Thermal analyses

TG measurements were performed under a synthetic air flow (60 ml min^{-1}) at a heating rate of 10 °C min^{-1} on a Setaram Labsys TG-TDA 12 thermogravimetric analyzer.

Acknowledgements

This work was supported by the Spanish government under MAT 2002-0043, the Generalitat de Catalunya under XI2002-9 and the EU under the project Nanomagiqc. P. G. is grateful to the Région Languedoc-Roussillon for their financial support. D. R.-M. also wants to thank Prof. David Hendrickson for fruitful discussions on the chemistry of Mn_{12} clusters.

† CCDC reference numbers 231113–231115. See http://www.rsc.org/suppdata/nj/b4/b411371c/ for crystallographic data in .cif or other electronic format.

References

1 (*a*) G. Christou, D. Gatteschi, D. N. Hendrickson and R. Sessoli, *MRS Bull.*, 2000, **25**, 56; (*b*) D. Gatteschi and R. Sessoli, *Angew. Chem., Int. Ed.*, 2003, **42**, 268.
2 C. Boskovic, W. Wernsdorfer, K. Folting, J. C. Huffman, D. N. Hendrickson and G. Christou, *Inorg. Chem.*, 2002, **41**, 5107 and references therein.
3 C. Cadiou, M. Murrie, C. Paulsen, V. Villar, W. Wernsdorfer and R. E. P. Winpenny, *Chem. Commun.*, 2001, 2666.
4 E. C. Yang, D. N. Hendrickson, W. Wernsdorfer, M. Nakano and G. Christou, *J. Appl. Phys.*, 2002, **91**, 7382.
5 (*a*) C. Sangregorio, T. Ohm, C. Paulsen, R. Sessoli and D. Gatteschi, *Phys. Rev. Lett.*, 1997, **78**, 4645; (*b*) A. L. Barra, A. Caneschi, A. Cornia, F. F. De Biani, D. Gatteschi, C. Sangregorio, R. Sessoli and L. Sorace, *J. Am. Chem. Soc.*, 1999, **121**, 5302.
6 J. J. Sokol, A. G. Hee and J. R. Long, *J. Am. Chem. Soc.*, 2002, **124**, 7656.
7 D. Ruiz-Molina, G. Christou and D. N. Hendrickson, *Mol. Cryst. Liq. Cryst.*, 2000, **343**, 17.
8 M. Soler, W. Wernsdorfer, Z. Sun, J. C. Huffman, D. N. Hendrickson and G. Christou, *Chem. Commun.*, 2003, 2672.
9 A. Cornia, A. C. Fabretti, R. Sessoli, L. Sorace, D. Gatteschi, A. L. Barra, C. Daiguebonne and T. Roisnel, *Acta Crystallogr., Sect. C*, 2002, **58**, m371.
10 P. Gerbier, D. Ruiz-Molina, N. Domingo, D. B. Amabilino, J. Vidal-Gancedo, J. Tejada and J. Veciana, *Monatsch, Chem.*, 2003, **134**, 265.
11 G. Christou, *Acc. Chem. Res.*, 1989, **22**, 328.
12 Similar isomeric forms of Mn_{12} with a 1 : 1 : 2 disposition of the coordinating water molecules have already been described in the literature, as confirmed by a search on the *CSD Crystallographic Database*, version 5.24, updates April 2003.
13 (*a*) J. B. Vincent, H. R. Chang, K. Folting, J. C. Huffman, G. Christou and D. N. Hendrickson, *J. Am. Chem. Soc.*, 1987, **109**, 5703; (*b*) Z. J. Zhong, J. Q. Tao, H. Li, X.-Z. You and T. C. W. Mak, *Polyhedron*, 1997, **16**, 1719 and references therein.
14 A. R. Schake, J. B. Vincent, Q. Li, P. D. W. Boyd, K. Folting, J. C. Huffman, D. N. Hendrickson and G. Christou, *Inorg. Chem.*, 1989, **28**, 1915.
15 During the submission of this work, we have found that two isomeric forms of complex **2** have been simultaneously published: H. Zhao, C. P. Berlinguette, J. Bacsa, A. V. Prosvirin, J. K. Bera, S. E. Tichy, E. J. Schelter and K. R. Dunbar, *Inorg. Chem.*, 2004, **43**, 1359. One of these isomers exhibits similar magnetic properties and structural characteristics as complex **6**. On the contrary, the second isomeric form displays a considerably lower thermal barrier for magnetic relaxation due to the lower site symmetry of the Mn(III) ions and the canted orientations of two of the Jahn–Teller axes.
16 F. Luis, F. L. Mettes, J. Tejada, D. Gatteschi and L. J. de Jongh, *Phys. Rev. Lett.*, 2000, **85**, 4377 and references therein.
17 J. K. McCusker, H. G. Jang, S. Wang, G. Christou and D. N. Hendrickson, *Inorg. Chem.*, 1992, **31**, 1874.
18 The thermal behaviour of complex **6** under an argon atmosphere as already been described: J. Larionova, R. Clérac, B. Boury, J. Le Bideau, L. Lecren and S. Willemein, *J. Mater. Chem.*, 2003, **13**, 795.
19 The high solubility of complex **1** has so far prevented us to obtaining single crystals suitable for X-ray structure resolution. Therefore, its structure was simulated and optimized using the program *Hyperchem QSAR Properties Software*, V7.5, Hypercube, Inc.
20 X-Ray crystallographic data for complex **6** were obtained from the *CSD Crystallographic Database*, version 5.24, updates April 2003.
21 Spontaneous fragmentation of Mn_{12} complexes to yield lower nuclearity clusters, even at room temperature, has already been described: P. Gerbier, D. Ruiz-Molina, J. Gomez, K. Wurst and J. Veciana, *Polyhedron*, 2003, **22**, 1951.
22 These results diverge from the work developed by Winpenny *et al.* who demonstrated that the use of sterically hindered carboxylates ligands is a successful synthetic approach to obtain novel structures with higher nuclearities: A. Graham, S. Meier, S. Parsons and R. E. P. Winpenny, *Chem. Commun.*, 2000, 811.
23 *SAINT*, v. 4.050, Brucker Analytical X-ray Instruments, Inc., Madison, WI, 1998.
24 *SHELXTL*, v. 5.030, Brucker Analytical X-ray Instruments, Inc., Madison, WI, 1998.